J Mol Model (2011) 17:1283–1294
DOI 10.1007/s00894-010-0831-4

ORIGINAL PAPER

Comparative analysis of receptor binding by chicken and human interleukin-1β

Chao-Sheng Cheng · Wen-Shiang Lu · I-Fan Tu · Ping-Chiang Lyu · Hsien-Sheng Yin

Received: 29 June 2010 / Accepted: 22 August 2010 / Published online: 5 September 2010

Abstract Interleukin-1β (IL-1β) is an important cytokine in the immune system. Mammalian and avian IL-1βs share only 31-35% sequence identity, and the function of avian IL-1βs is less well understood by comparison. Although chicken and mammalian IL-1βs have similar tertiary structures, these ILs differ significantly with respect to receptor activation. Analysis of the structures and sequences of IL-1βs reveals that the major differences lie in loops. Modeling docking of chicken IL-1β to its receptor reveals that these variable loops are critical for receptor binding. Molecular dynamics simulations of the IL-1βs reveal significant changes in the dynamic range of motion upon receptor binding. Loops 3 and 9 of the unbound chicken IL-1β had greater fluctuations compared with the other loops. Upon binding, the flexibility of these loops, which directly contact the receptor, markedly decreases. Taken together, these results suggest that receptor binding leads to not only favorable enthalpy but also lower conformational entropy.

Keywords Chicken interleukin-1β · Homology modeling · Molecular docking · Molecular dynamics · Type I interleukin-1 receptor

Introduction

Interleukin-1 (IL-1) is an important proinflammatory cytokine linked to host defense in the innate immune system [1, 2]. The IL-1 family comprises two receptor agonists, IL-1α and IL-1β, and a specific antagonist, IL-1 receptor antagonist (IL-1Ra) [1]. In humans, the biological properties of IL-1, especially IL-1β, are well studied [3–7]. IL-1β is produced by macrophages, monocytes, neutrophils, hepatocytes and other cells [2] and has been shown to mediate autoinflammatory diseases [8]. In both mammalian and avian cells, IL-1β can enhance production of immune-related molecules, such as adrenocorticotropin, nitric oxide, acute-phase proteins, cytokines and chemokines, and thus trigger an immune response [9–12]. More recently, IL-1β has been considered as a potential therapeutic target for the treatment of pain in animals and humans [13].

Three-dimensional (3D) structures of human and murine IL-1βs have been determined by X-ray crystallography [14–16]. These two structures share high sequence identity (72%) and a similar structural fold [14], comprising 12-14 β-strands and 1-2 α-helices. The β-strands form an antiparallel β-barrel, with a shallow open face at one end and a closed face at the other. Recently, IL-1βs from avian species (chicken, duck, goose, turkey and pigeon) have been cloned and characterized [11, 17]. The sequence identity among avian species is more than 78%. However, the avian and mammalian IL-1βs share only 31-35% sequence identity (Fig. 1). The most highly conserved residues in the avian and mammalian IL-1βs are located in β-strands, implying that the secondary structural elements in IL-1βs are highly conserved. In addition, IL-1βs from avian species contain an insertion of five amino acid residues (PRGPR) at positions 53-57. Residues in this region of human IL-1β are reportedly critical for receptor binding [18]. Other receptor binding sites in human IL-1β, highlighted in gray in Fig. 1, are highly conserved among mammals but are quite different compared to avian IL-1βs. On the other hand, species cross-reactivity shows that chicken IL-1β only weakly activates the receptor on murine

C.-S. Cheng · W.-S. Lu · I.-F. Tu · P.-C. Lyu · H.-S. Yin (✉)
Institute of Bioinformatics and Structural Biology and College of Life Sciences, National Tsing Hua University,
No. 101, Section 2, Kuang-Fu Road,
Hsinchu, Taiwan 30013
e-mail: hsyin@life.nthu.edu.tw

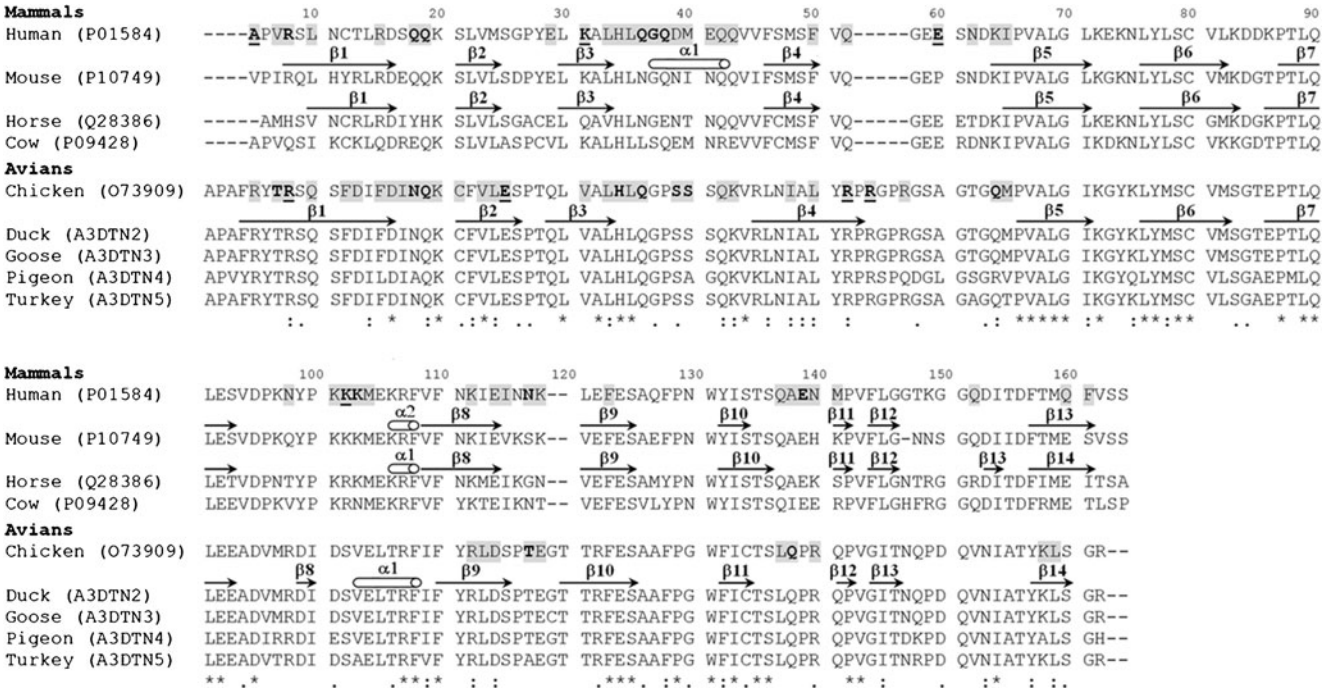

Fig. 1 Multiple sequence alignment for mammalian and avian IL-βs. The sequences of the mature forms of IL-1βs were retrieved from ExPASy, and their accession numbers are indicated in parentheses. Identical (*), conserved (:) and semi-conserved (.) residues are identified. Residues directly involved in receptor binding are shaded in gray, and their interaction with the receptor is denoted as via hydrogen-bonding (bold) or salt bridge (underline). The locations of β-strands and α-helices are indicated by arrows and cylinders, respectively

thymocytes and that human and murine IL-1βs do not activate the receptor on chicken thymocytes [19]. These results suggest that IL-1βs from avians and mammals activate their receptors in a highly species-specific manner.

To understand the role and significance of heterologous IL-1βs, we compared structural properties of chicken IL-1β with those of murine and human IL-1βs. Additionally, molecular docking and molecular dynamics (MD) simulations were used to explore receptor binding of chicken IL-1β. We anticipate this study will expand our understanding of IL-1β function in the immunological response.

Methods

Structural comparison of mammalian and avian IL-1βs

Protein sequences were retrieved from ExPASy Molecular Biology Server (http://ca.expasy.org/) and aligned with the aid of ClustalW (http://www.ebi.ac.uk/clustalw) [20]. The crystal structures of murine IL-lβ (PDB entry 2MIB, 2.8 Å resolution) [14] and human IL-lβ (PDB entry 9ILB, 2.28 Å resolution) [15] were superimposed with the chicken IL-lβ structure (PDB entry 2WRY, 1.58 Å resolution) (unpublished data) using Swiss-PdbViewer v3.6 [21] and Discovery Studio 2.0 (Accelrys Inc., San Diego, CA). The backbone atomic root mean square deviation (rmsd) values were also measured. Hydrogen bond (HB) networks were generated using HB plot (http://www.virtuadrug.com/hbplot) [22]. PyMOL was used for molecular visualization and representation of the electrostatic potential surface map [23, 24].

Molecular modeling and receptor docking of chicken IL-1β

Homology modeling was used to construct a 3D model for the structure of the extracellular domain of chicken type I IL-1 receptor (IL-1R type I) using the structure of human IL-1R type I (PDB entry 1ITB) as the template [18]. Protein sequences were aligned using ClustalW [20], with 35% sequence identity and an E-value of $2e^{-52}$, and the molecular model was generated using Modeller 6v2 [25–27]. The initial model was optimized using the CHARMM [28] force-field and a steepest descent minimization protocol in the Discovery Studio software. Protein secondary structure was assigned by DSSP [29] and STRIDE [30]. Structure validation was performed by PROCHECK v.3.5.4 [31], ProQ (http://www.sbc.su.se/~bjornw/ProQ/) [32] and MetaMQAPII (https://genesilico.pl/toolkit/) [33].

The chicken IL-1β structure was docked to IL-1R type I using PatchDock [34] docking program. The program automatically docks IL-1β into the active site of IL-1R

type I in all possible orientations. Using the PatchDock algorithm, the geometric hashing and pose-clustering matching techniques were applied to match the shape, and the clustering rmsd was set to 4.0 Å. The best-ranked 30 docked poses were evaluated and visually inspected. The pose with the most favorable energy and the lowest rmsd value compared to human IL-1R type I–IL-1β complex was selected as our model for the complex, and was further refined by MD simulations.

MD simulations for the IL-1β–IL-1R type I complex

Chicken IL-1β and IL-1R type I in both free and complexed forms were used for the simulation studies using the Gromacs 3.3 package [35]. All missing hydrogen atoms were added using the GROMOS96 43a1 force field [36]. Water molecules in the crystal structure were retained for the simulation. Starting structures in the free or complexed forms were individually immersed into a rectangular box containing pre-equilibrated single-point charge water models [37] with 12 Å as the shortest distance between the box edge and the solutes. This resulted in ~9,500 water molecules in the simulation box for chicken IL-1β, ~23,000 waters for IL-1R type I alone and the IL-1R type I–IL-1β complex. To achieve electro-neutrality, single–point charge water molecules were randomly replaced with eight and six sodium ions (Na^+) for IL-1R type I and the IL-1R type I–IL-1β complex, respectively, and with two chloride ions (Cl^-) for free IL-1β.

The MD simulations began with steepest descent energy minimization for 100 ps to relax any steric conflicts in the initial systems. Subsequently, MD simulations were performed using decreasing positional restraints in order to equilibrate the systems. After equilibration, all systems were simulated over 7 ns in the isobaric-isothermal ensemble (the NpT ensemble) using periodic boundary conditions. The temperature was maintained by coupling the protein, solvent, and counter-ions to a reference temperature bath at 300 K with a coupling constant τ_t of 0.1 ps [38]. The pressure was controlled using Berendsen's weak-coupling algorithm set at one atmosphere pressure with a coupling constant τ_p of 0.5 ps [38]. Lennard-Jones interactions were truncated at a cut-off distance of 12 Å. Long-range electrostatic interactions were modeled using the particle mesh Ewald algorithm [39]. The linear constraint solver (LINCS) algorithm was used to restrain all bond lengths [40]. The integration time step was 2 fs, and the coordinates of individual systems were collected every 0.5 ps during the production runs. For the complex structure, ten snapshots taken randomly from the final 3 ns of the production run were used to analyze the protein-protein interactions using Discovery Studio and LIGPLOT v.4.0 software [41].

Results and discussion

Comparison of mammalian and avian crystal structures

According to previous results from a species cross-activation study [19], chicken and mammalian IL-1βs exhibit significantly different bioactivities on thymocytes. The 3D structure of chicken IL-1β was first compared to that of human and murine IL-1βs (Fig. 2). These structures share a very similar structural fold, with rmsd values for chicken IL-1β compared to human and murine IL-1βs are 4.20 Å and 4.02 Å, respectively. The antiparallel β-strands show especially good superimposition, although close examination reveals significant differences in the N- and C-termini and in loops 3, 4, 7, 8, and 9. Loop 3 (residues 34-44) in chicken IL-1β is of similar length to the equivalent loop in each of the other two IL-1βs, but the structures do not superimpose well. Human IL-1β has a short helical segment in this region that is not present in

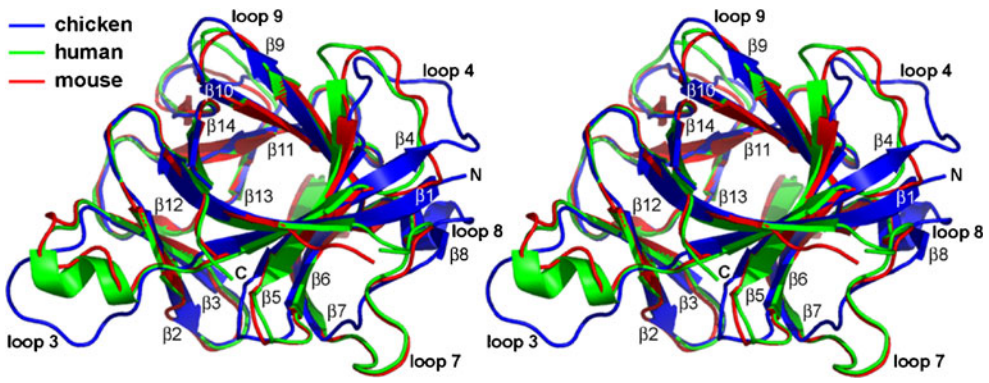

Fig. 2 Cartoon representation of structural comparison among IL-1βs. The structures of chicken (blue), mouse (red), and human (green) IL-1βs are superimposed and presented in stereo. β-strands are numbered sequentially and represented by twisted arrows. The N-terminus (N) and C-terminus (C) are indicated. Loops connecting β-strands are named according to which strands they connect

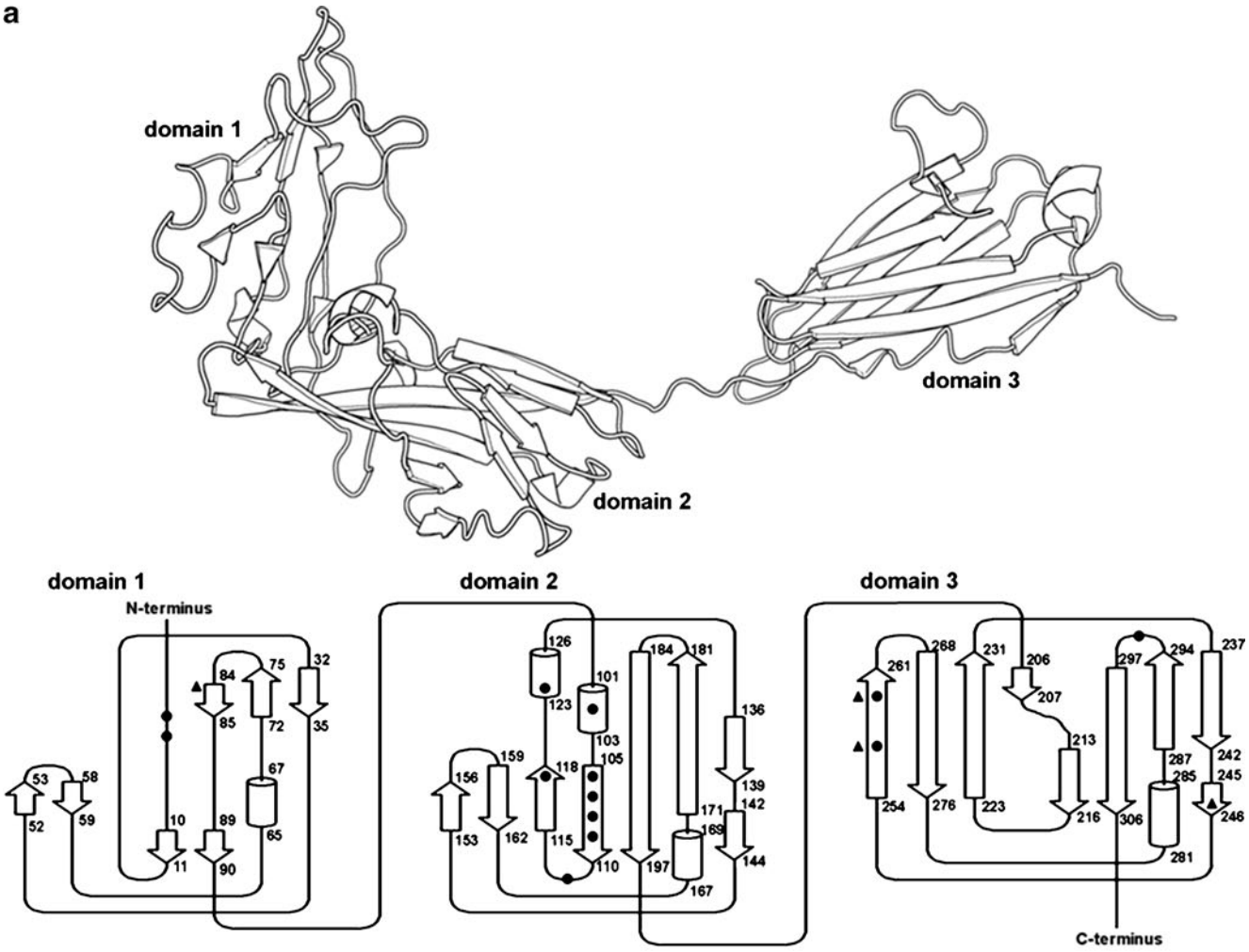
a
domain 1
domain 2
domain 3
N-terminus
C-terminus

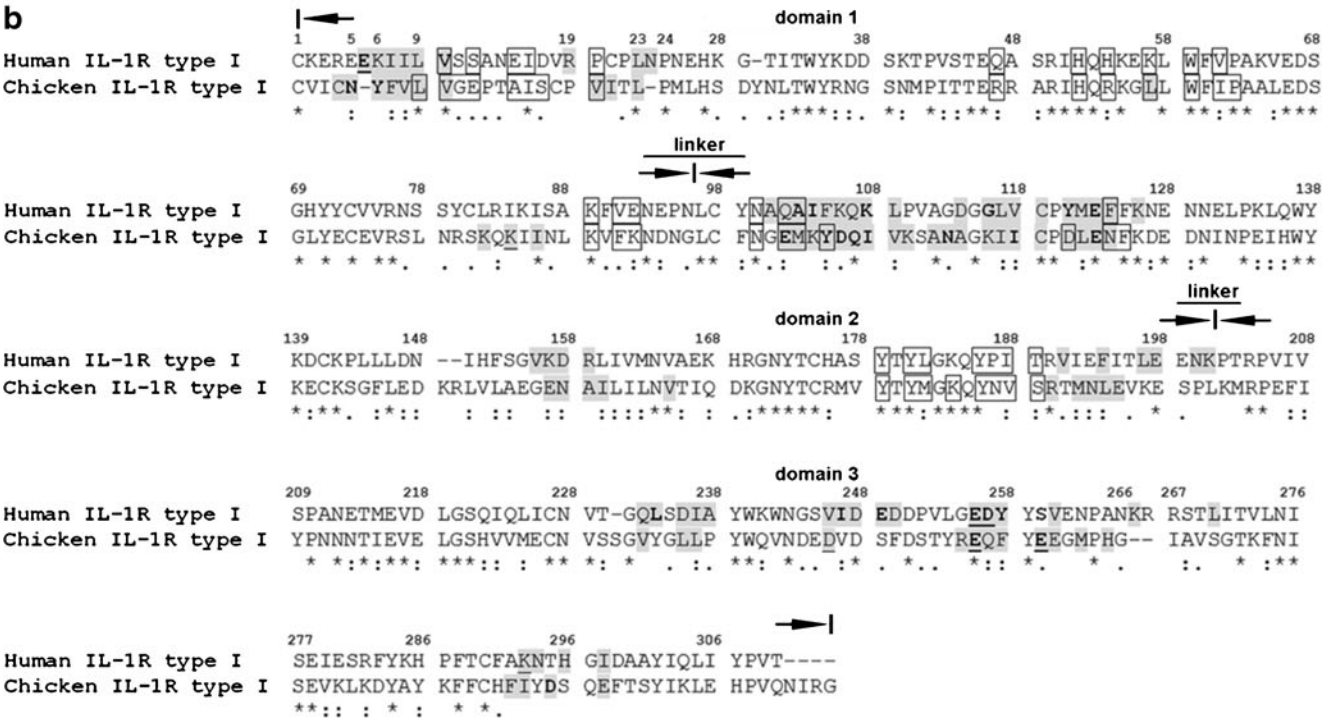
b
domain 1
linker
domain 2
linker
domain 3
Human IL-1R type I
Chicken IL-1R type I

◀ **Fig. 3** Schematic representation of the structure of chicken IL-1R type I. (**a**) A ribbon representation of the 3D structure and a topology diagram of chicken IL-1R type I are shown, with the three domains indicated. Hydrogen bonds and salt bridges across the protein-protein interface are denoted as black circles and triangles, respectively. (**b**) Sequence alignment for the human and chicken receptors. The location of the domains and linker regions are labeled in the figure. Gray shading indicates residues that are directly involved in the binding of IL-1β. Residues involved in hydrogen bonds and salt bridges with IL-1β are indicated by bold and underlined letters, respectively. Rectangle box indicates residues that are involved in the inter-domain contacts. Identical (*), conserved (:) and semi-conserved (.) residues are also identified

chicken IL-1β. The sequence PSSS (residues 38-41) in avian species differs from that in mammalian sequences, which likely explains the structural difference. Loop 4 (residues 54-65) exhibits considerable conformational variability; indeed chicken IL-1β has five additional residues inserted here that extend the length of Loop 4. This insertion alters the conformation and increases the local rmsd value. Of particular interest is the conformation of residues 94-109 (loops 7 and 8) in chicken IL-1β. In this region, chicken IL-1β has a distinctly different structure, with an additional β-strand and a longer helical segment. Comparing the sequences in Fig. 1, mammalian IL-1βs have a highly conserved sequence between residues 96 and 106 of P(K/N)XYPK(K/R)(K/N)MEK, which is not found in chicken IL-1β. Two unique proline residues (Pro96 and Pro100) in mammalian IL-1βs probably contribute the differences in this loop region. All of the regions of differences lie at identified binding sites for human IL-1β [42]; it is therefore likely that these two IL-1βs bind to their respective receptors via distinct interactions.

Molecular modeling of chicken IL-1R type I

To gain insight into the mechanism by which chicken IL-1β binds to its receptor, a 3D structural model for chicken IL-1R type I was constructed by homology modeling of the chicken sequence based on a known structure of human IL-1R type I. The folding of the extracellular domain of chicken IL-1R type I is similar to that of the human receptor [18, 43]. Chicken IL-1R type I has three well-defined immunoglobulin-like domains: domain 1 (residues 1-96), domain 2 (residues 97-201) and domain 3 (residues 202-310). All domains are predominantly β-strand, as they

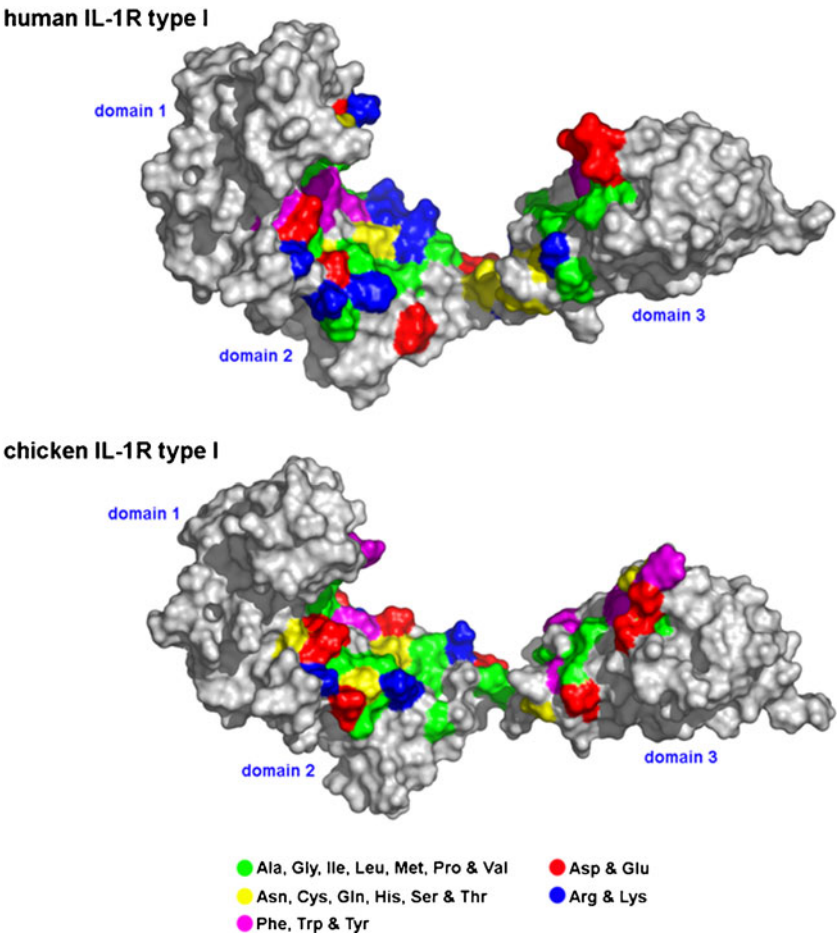

Fig. 4 Surface maps of human and chicken IL-1R type Is. Nonpolar aliphatic residues (green), aromatic residues (magenta), polar uncharged residues (yellow), positively charged residues (blue), and negatively charged residues (red) of human IL-1R type I that are directly involved in interactions with IL-1β are shown. Amino acids of chicken IL-1R type I at the corresponding positions in the human receptor, based on the sequence alignment, are also shown

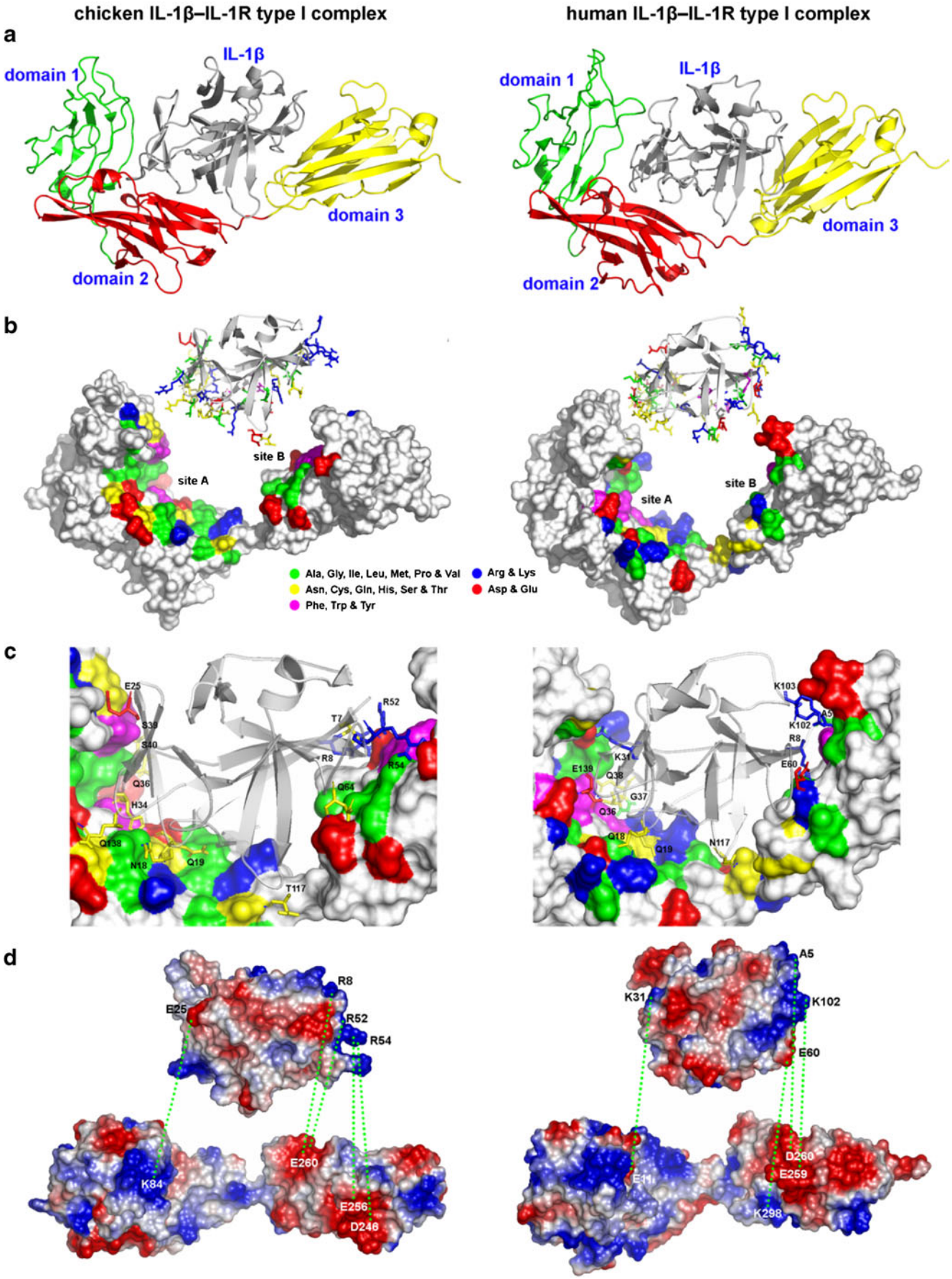
chicken IL-1β–IL-1R type I complex
human IL-1β–IL-1R type I complex
a
IL-1β
domain 1
domain 2
domain 3
b
site A
site B
Ala, Gly, Ile, Leu, Met, Pro & Val
Asn, Cys, Gln, His, Ser & Thr
Phe, Trp & Tyr
Arg & Lys
Asp & Glu
c
E25
S39
S40
Q36
H34
Q138
N18
Q19
T7
R52
R8
R54
Q64
T117
K103
A5
K102
R8
K31
E139
Q38
G37
Q36
Q18
Q19
N117
E60
d
R8
E25
R52
R54
K84
E260
E256
D248
A5
K31
K102
E60
E11
D260
E259
K298

◀ **Fig. 5** Structural model of IL-1β binding to its receptor, IL-1R type I. (**a**) Ribbon representation of the IL-1β–IL-1R type I complex, with the three domains of IL-1R type I labeled in different colors. (**b**) The receptor-bound complex of IL-1β (ribbon representation) and IL-1R type I (surface model) showing the residues involved in protein-protein interactions in IL-1β (sticks) and IL-1R type I (colored surfaces). Binding sites A and B in the receptor are also indicated. (**c**) Hydrogen bonds across the binding interface, labeled and represented as blue dashed lines. (**d**) Electrostatic potential surface map showing charge-charge interactions and the specific residues involved in salt bridges

form a 7-strand β-barrel (Fig. 3). Domain l has a less highly ordered tertiary structure, and an HB plot reveals that indeed domain 1 has fewer HBs (data not shown). Compared to human IL-1R type I, domain 3 in chicken IL-1R type I is rotated outward by approximately 24°. Superposition of these two IL-1R type I structures yields a backbone rmsd value of 3.67Å. The first linker between domains 1 and 2 is conservatively substituted but it is not for the second linker (Fig. 3b). The residues involved in the domain-domain interactions are mostly conserved substituted, as shown with a rectangle box in Fig. 3b, but minor differences still can be seen at positions 15, 20, 57, 103, 124, and 187. These differences during the model construction probably alter flexibility among the domains. Validation of the chicken IL-1R structure using PROCHECK revealed that more than 98% of the amino acids had conformations that lie in allowed regions of the Ramachandran plot. The exceptions were Thr44, Ile61, Asp129 and Asp148; all of these residues are located in flexible turn or loop regions, which may increase the uncertainty in their positioning in the molecular model. ProQ and MetaMQAPII were also used to make an integrative assessment of the structure quality. The results show that LGscore of ProQ is 2.005 and GDT_TS of MetaMQAPII is 46.855, which indicates that our model is a fairly good model and has properly folded.

Previous studies have shown that human IL-1R type I has two conserved binding sites for IL-1β [18]. Site A lies at the junction between domains 1 and 2, and site B is on the face of domain 3 (Fig. 4). As is the case for human and chicken IL-1βs, the amino acid sequence at the binding sites of human IL-1R type I differ from those in chicken IL-1R type I. In site A, the human receptor has eight positively charged and five negatively charged residues that interact with IL-1β. In contrast, the corresponding site in the chicken receptor has only four positively charged but six negatively charged residues. The distribution of these charged residues also differs between the receptors. Additionally, the human site A has 16 non-polar aliphatic and four aromatic residues, whereas the chicken site A has 18 non-polar aliphatic and three aromatic residues. At site B, the main difference between the human and chicken receptors lies in the positively charged and aromatic residues: the human receptor has two positively charged residues whereas the chicken receptor has none, and the chicken receptor has two tyrosines and two phenylalanines whereas the human receptor has only one aromatic residue (tyrosine).

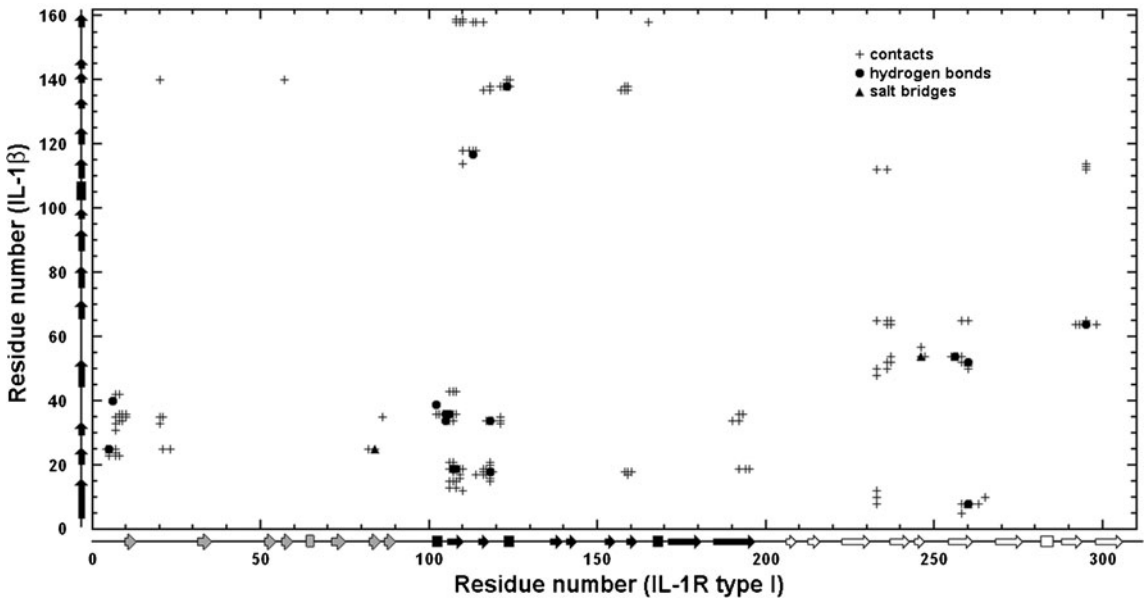

Fig. 6 Contact map for the IL-1β–IL-1R type I complex. Residues directly involved in contacts, hydrogen bonds, and salt bridges across the protein-protein interface are indicated. The locations of secondary structural elements in IL-1β and IL-1R type I are denoted along the axes by arrows (β-strands) and rectangles (α-helices). The three domains of IL-1R type I are indicated in light gray (domain 1), black (domain 2) and white (domain 3)

Molecular docking of chicken IL-1β to its receptor, IL-1R type I

The chicken IL-1β structure was docked to its receptor, IL-1R type I, to investigate potential binding modes (Fig. 5a). The chicken receptor has three domains that can wrap around IL-1β—similar to the model proposed for the human IL-1β–IL-1R type I complex [18]. The surface area of the binding interface is approximately 5,500 Å^2, calculated using UCSF Chimera [44] software. Like the human receptor, chicken IL-1R type I contains the binding sites A and B that make close contacts with IL-1β (Fig. 5b); the residues involved in these protein-protein interactions are shown in Fig. 6. The positions of these residues in chicken IL-1β and receptor are similar in 3D space to those in human, but there are substantial differences in the types of amino acids involved (Fig. 1, Fig. 3b, gray-highlighted residues). In site A, the non-polar residues of chicken IL-1β at F15, I17, V23, L24, V31, L33, L35, L137 and L159 form a hydrophobic patch that interacts with hydrophobic residues in the receptor (Fig. 5b). These highly conserved hydrophobic residues in avian IL-1βs are evenly distributed over the surface of domains 1 and 2. Compared to the chicken IL-1β–IL-1R type I complex structure, fewer hydrophobic interactions are observed in the human IL-1β–IL-1R type I complex, and most of these occur at the interface of domain 2 and IL-1β [18]. In addition, eight residues (positions 18, 19, 25, 34, 36, 39, 40, and 138) form HBs with the receptor (Fig. 5c, blue dashed lines). These residues are located mainly at the junction of domains 1 and 2, and this is similar to what is observed for human IL-1β [18]. However, these residues are conserved among avians (Fig. 1) but are quite different compared to mammalian IL-1βs. Of particular note is the negatively charged residue (Glu25) in chicken IL-1β that forms a critical salt bridge with Lys84 of the receptor (Fig. 5d); a similar interaction occurs in the human complex, but the polarity of the salt bridge is reversed [18]. Residues in β-strands β1, β2, β3, and β14 and in loops 1, 3, 9, and 11 in chicken IL-1β are able to make close contacts with the N-terminal regions of domains 1 and 2 of the receptor, thereby stabilizing these areas.

Five residues (F12, I48, L50, M65 and L113) of chicken IL-1β engage in hydrophobic interactions with the receptor site B. The distribution of these non-polar residues is more crowded than that in human IL-1β (Fig. 5b). According to sequence alignment (Fig. 1), all of these residues are conserved in avian IL-1βs. In addition, chicken IL-1β has three residues (Arg8, Arg52 and Arg54) that form salt bridges with receptor site B (Fig. 5d). Three salt bridges, at residues Ala5 (amine group), Glu60 and Lys102 of human IL-1β, are found in this region [18], but the polarity of one salt bridge is reversed (Glu60-Lys298). This indicates that electrostatic interactions and the locations of the charged residues involved at the interface of IL-1β and receptor help stabilize the complex. In addition, human and chicken IL-1βs have similar HB networks at the interfaces of their respective receptors.

MD simulations

To assess the quality of the MD simulations, we examined the rmsd values of all heavy atoms during the production

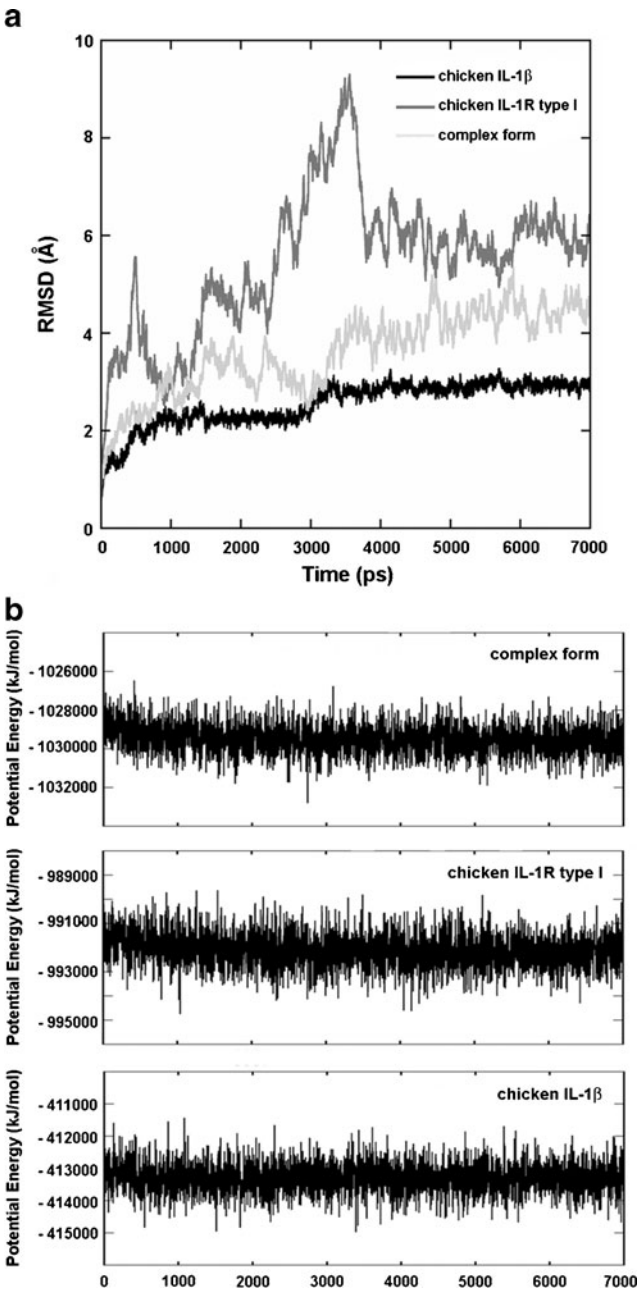

Fig. 7 Rmsd values (**a**) and potential energies (**b**) for chicken IL-1R type I and IL-1β in the free and complexed forms, plotted as a function of molecular dynamics simulation time

runs of the chicken IL-1β, the IL-1R type I, and the IL-1β–receptor complex (Fig. 7a). The results show that during the first 4 ns, the rmsd values have sizeable variations, with the receptor showing the greatest variation; thereafter, however, they reach equilibrium and remain stable. This indicates that the coordinates of the receptor have the largest atomic deviations. In addition, potential energies over the course of the MD simulations indicate that all simulated systems are stable (Fig. 7b); thus, three systems have converged to an equilibrium state in the simulations, and the final 3 ns can be used for the trajectory analysis.

The root mean square fluctuation (rmsf) for each residue was calculated for both free and receptor-bound IL-1β (Fig. 8). Lower rmsf values were observed in the secondary structural elements, indicating that these regions have smaller atomic fluctuations. Most of the residues in the receptor were stabilized upon association with IL-1β, except for Asn130, Asp148, Lys149 and Arg150, for which rmsf values were greater than 2.9 Å—these residues are not close to the binding sites and lie in loops, thus having fewer HB constraints to limit their flexibility. The receptor residues directly involved in interactions with IL-1β (denoted by + in Fig. 8) have clearly lower rmsf values. On the other hand, the receptor in the unassociated form has lower average rmsf values at the conserved participating junction residues (1.66 Å) and the linker between domains 1 and 2 (1.88 Å), where the average rmsf value for entire protein is 2.29 Å. However, the non-conservatively substituted linker between domains 2 and 3 has a higher rmsf value of 2.50 Å. This indicates that, during model construction, non-conserved residue substitution at domain interface can affect protein flexibility. To visualize structural fluctuations, a "sausage" diagram is used to demonstrate the range of observed motions during simulation trajectories (Fig. 9a), and a thicker sausage tube denotes a more mobile region. In the free form of IL-1R type I, increased mobility is observed in three regions, labeled A, B, and C in Fig. 9a,b. Regions A and C are at the edge of two binding sites, and these regions have fewer constraints. The average all-atom rmsd values of regions A and C in the unassociated form are 7.27 Å and 9.55 Å, respectively, which are higher than that of the entire protein (6.38 Å). Region B is located at the junction between domains 2 and 3—this may serve as a "hinge" to control the opening or closing of these domains. The average rmsd value for this region is 6.02 Å. Upon IL-1β binding, the range of motions in the entire receptor appears to decrease, especially at the binding sites, indicating that interactions with IL-1β can significantly alter the mobility of residues internal to the receptor.

For IL-1β, the rmsf values in both the free and receptor-bound forms appear to be lower than those in the receptor, implying that IL-1β has relatively smaller atomic fluctuations compared to the receptor (Fig. 8b). Lower rmsf values are mostly observed in the secondary structural elements due to HB constraints. Loops 3, 4, 5, 6, 7, and 9 in free IL-1β have greater rmsf values and atomic fluctuations. Upon binding to the receptor, rmsf values for IL-1β increase slightly, particularly for residues 55-61, 84 and 85; these nine residues have the largest rmsf values (>2.0 Å).

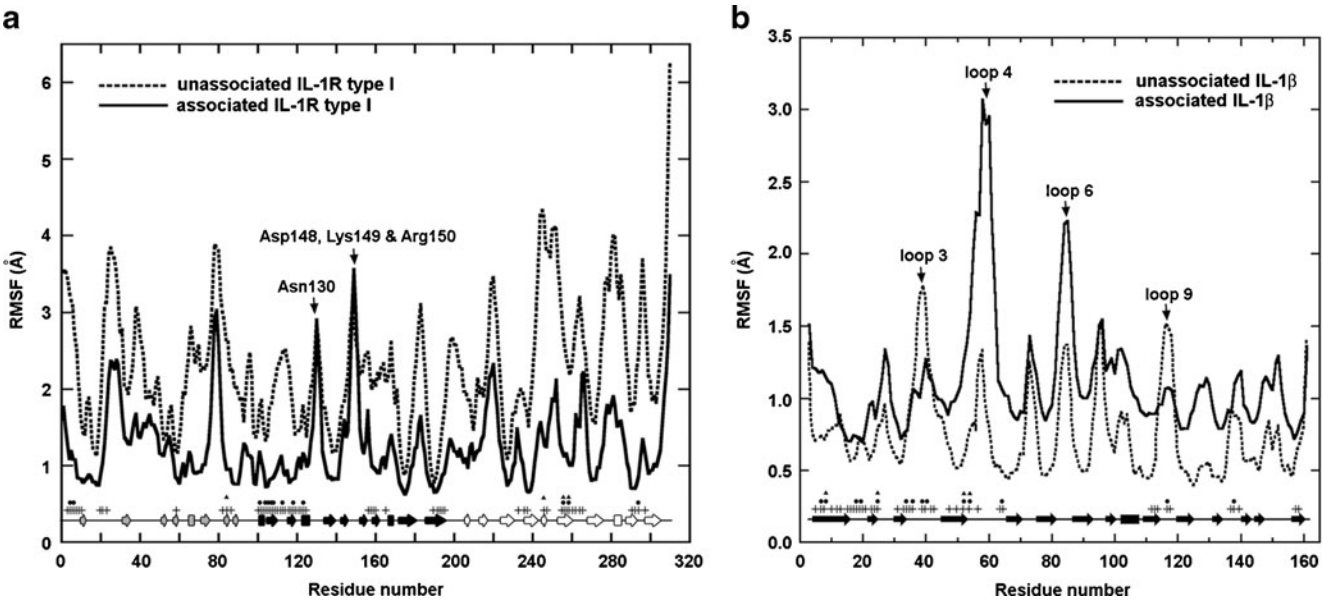

Fig. 8 Rmsf values as a function of amino acid sequence for IL-1R type I (**a**) and IL-1β (**b**) in the free (unassociated) and complexed (associated) forms. The locations of secondary structural elements in IL-1β and IL-1R type I are denoted along the *x*-axis by arrows (β-strands) and rectangles (α-helices). Residues involved in interactions across the binding interface are indicated: close contacts (crosses), hydrogen bonds (circles), and salt bridges (triangles). The three domains of IL-1R type I are labeled in different colors

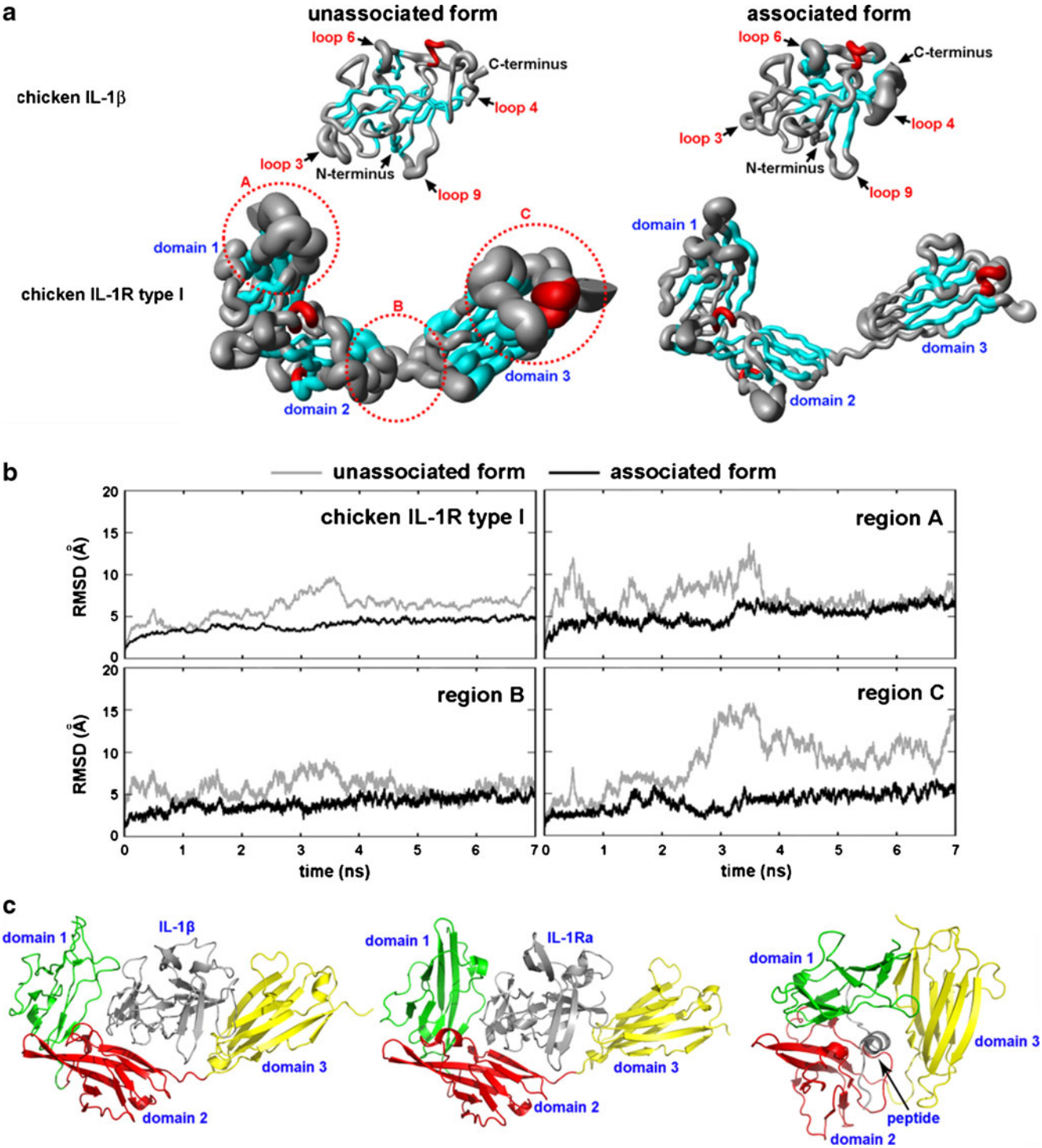

Fig. 9 Structural representation of MD simulations of the IL-1β–IL-1R type I complex. (**a**) A "sausage" view illustrates the observed range of motions during simulations. The coordinates of individual systems were collected every 10 ps during the final 3 ns of simulation and overlaid using Molmol [47]. The thickness of the backbone reflects the mobility of the region. The most mobile regions in the unassociated form of chicken IL-1R type I are indicated by dashed red circles. (**b**) MD trajectories of rmsd values of three mobile regions (A, B and C). A rmsd plot calculated with all-atoms is present, where the gray line represents the unassociated form, and the dark line represents the associated form. (**c**) Human IL-1R type I complexed with three different interacting ligands: the IL-1R type I agonist IL-1β, the antagonist IL-1Ra, and antagonist AF10847. IL-1R type I domains 1, 2 and 3 are shown in green, red and yellow, respectively

Residues 55-61 (GPRGSAG) in loop 4 have fewer restraints in the crystal structure, and after receptor binding most of these residues do not participate in interactions with receptor; the three G residues in this sequence probably enhance mobility. A similar phenomenon is seen for residues 84 and 85. Upon receptor binding, residues in IL-1β loops 3 and 9 have decreased rmsf values, as indicated by a thicker sausage tube for the polypeptide chain in Fig. 9a. Our docking results show that these two loops may be involved in receptor binding. Upon binding to receptor, these loops help to constrain the movement of segments in the receptor, effectively decreasing the receptor's internal mobility. Moreover, these loops have two unique proline residues (Pro38 and Pro116) in avian IL-1βs. Although these two residues do not interact with the receptor, they probably have the different effect of loop flexibility compared with mammalian IL-1βs. A similar phenomenon is seen for Pro139. Other residues that make contact with the receptor have lower rmsf values (thinner tubes in Fig. 9). This indicates that interactions between IL-1β and IL-1R type I require favorable contacts (enthalpic component) and a decrease in conformational flexibility upon complex formation (entropic component) [45].

In the human IL-1β–IL-1R type I complex (Fig. 9c), the receptor must have substantial flexibility, especially in regions A, B and C, to accommodate ligands such as IL-1β [18] and peptide AF10847 [46]. Upon binding of human IL-1β, the conformation of the entire receptor changes significantly, thereby promoting the binding of the IL-1R type I accessory protein and activating signal transduction from the receptor [43]. Human IL-1Ra, an IL-1 receptor–specific antagonist, is also capable of interacting with human IL-1R type I [43]. Although IL-1Ra and IL-1β have similar structures, IL-1Ra is unable to induce the marked conformational changes in receptor domain 3, which are necessary for receptor activation, due to limited favorable contacts. This inhibits the association of the IL-1R type I accessory protein with the IL-1β–IL-1R type I complex for triggering the IL-1β-mediated immune response. Therefore, dynamic properties and favorable contacts at the IL-1β binding sites play an indispensable role in IL-1 biological function.

Conclusions

Although the crystal structure of chicken IL-1β shows that this IL has a similar tertiary structure to mammalian IL-1βs, close examination reveals significant differences in the structures of the N-terminus and certain loop regions. These variable regions have been shown to be critical for receptor binding. Results from ligand-receptor docking simulations indicate that chicken IL-1β binds to its receptor in a manner similar to that proposed for the human IL-1β–IL-1R type I complex. Amino acids within the regions that bind to the receptor are very different between chicken and human IL-1βs. Antisera against chicken IL-1β has been shown to neutralize IL-1βs from other avian species but not those from mammals [11]. The variable loops, therefore, may contribute to a wide variety of species-specific binding and cellular activities. Our MD simulations show that chicken IL-1R type I exhibits significantly different dynamic properties before and after IL-1β binding. We therefore hypothesize that, in the unliganded form, the receptor must have substantial flexibility so that it may alter its conformation to accommodate IL-1β binding. After IL-1β binding, the receptor's intrinsic mobility diminishes, thereby ensuring a tight interaction with the ligand. Finally, because IL-1β function is critical to innate immunity, protein engineering based on IL-1β structural information may yield a modified IL-1β having potential therapeutic applications for the treatment of pain in animals and humans.

Acknowledgments The authors acknowledge the support of the National Science Council, Taiwan (NSC grant numbers NSC-96-2311-B-007-015-MY3). Portions of this research were carried out at the National Synchrotron Radiation Research Center, a national user facility supported by the National Science Council of Taiwan, ROC.

References

1. Dinarello CA (2009) Immunological and inflammatory functions of the interleukin-1 family. Annu Rev Immunol 27:519–550
2. Arend WP, Palmer G, Gabay C (2008) IL-1, IL-18, and IL-33 families of cytokines. Immunol Rev 223:20–38
3. Nakae S, Asano M, Horai R, Iwakura Y (2001) Interleukin-1 beta, but not interleukin-1 alpha, is required for T-cell-dependent antibody production. Immunology 104:402–409
4. Dinarello CA (2007) Mutations in cryopyrin: bypassing roadblocks in the caspase 1 inflammasome for interleukin-1beta secretion and disease activity. Arthritis Rheum 56:2817–2822
5. Krelin Y, Voronov E, Dotan S, Elkabets M, Reich E, Fogel M, Huszar M, Iwakura Y, Segal S, Dinarello CA, Apte RN (2007) Interleukin-1beta-driven inflammation promotes the development and invasiveness of chemical carcinogen-induced tumors. Cancer Res 67:1062–1071
6. Fantuzzi G, Zheng H, Faggioni R, Benigni F, Ghezzi P, Sipe JD, Shaw AR, Dinarello CA (1996) Effect of endotoxin in IL-1 beta-deficient mice. J Immunol 157:291–296
7. Faggioni R, Fantuzzi G, Fuller J, Dinarello CA, Feingold KR, C. G (1998) IL-1β mediates leptin induction during inflammation. Am J Physiol 274:204–208
8. Dinarello CA (2009) Interleukin-1beta and the autoinflammatory diseases. N Engl J Med 360:2467–2470
9. Dinarello CA (1996) Biologic basis for interleukin-1 in disease. Blood 87:2095–2147
10. Introna M, Breviario F, d'Aniello EM, Golay J, Dejana E, Mantovani A (1993) IL-1 inducible genes in human umbilical vein endothelial cells. Eur Heart J 14:78–81

11. Wu YF, Liu HJ, Chiou SH, Lee LH (2007) Sequence and phylogenetic analysis of interleukin (IL)-1beta-encoding genes of five avian species and structural and functional homology among these IL-1beta proteins. Vet Immunol Immunopathol 116:37–46
12. Sick C, Schneider K, Staeheli P, Weining KC (2000) Novel chicken CXC and CC chemokines. Cytokine 12:181–186
13. Ren K, Torres R (2009) Role of interleukin-1beta during pain and inflammation. Brain Res Rev 60:57–64
14. van Oostrum J, Priestle JP, Grutter MG, Schmitz A (1991) The structure of murine interleukin-1 beta at 2.8Å resolution. J Struct Biol 107:189–195
15. Yu B, Blaber M, Gronenborn AM, Clore GM, Caspar DL (1999) Disordered water within a hydrophobic protein cavity visualized by X-ray crystallography. Proc Natl Acad Sci USA 96:103–108
16. Finzel BC, Clancy LL, Holland DR, Muchmore SW, Watenpaugh KD, Einspahr HM (1989) Crystal structure of recombinant human interleukin-1 beta at 2.0Å resolution. J Mol Biol 209:779–791
17. Weining KC, Sick C, Kaspers B, Staeheli P (1998) A chicken homolog of mammalian interleukin-1 beta: cDNA cloning and purification of active recombinant protein. Eur J Biochem 258:994–1000
18. Vigers GP, Anderson LJ, Caffes P, Brandhuber BJ (1997) Crystal structure of the type-I interleukin-1 receptor complexed with interleukin-1beta. Nature 386:190–194
19. Klasing KC, Peng RK (1987) Influence of cell sources, stimulating agents, and incubation conditions on release of interleukin-1 from chicken macrophages. Dev Comp Immunol 11:385–394
20. Thompson JD, Higgins DG, Gibson TJ (1994) Clustal W: improving the sensitivity of progressive multiple sequence alignment through sequence weighting, position-specific gap penalties and weight matrix choice. Nucleic Acids Res 22:4673–4680
21. Guex N, Peitsch MC (1997) SWISS-MODEL and the Swiss-PdbViewer: an environment for comparative protein modeling. Electrophoresis 18:2714–2723
22. Bikadi Z, Demko L, Hazai E (2007) Functional and structural characterization of a protein based on analysis of its hydrogen bonding network by hydrogen bonding plot. Arch Biochem Biophys 461:225–234
23. DeLano WL (2002) The PYMOL molecular graphics system. DeLano Scientific, San Carlos
24. Baker NA, Sept D, Joseph S, Holst MJ, McCammon JA (2001) Electrostatics of nanosystems: application to microtubules and the ribosome. Proc Natl Acad Sci USA 98:10037–10041
25. Marti-Renom MA, Stuart AC, Fiser A, Sanchez R, Melo F, Sali A (2000) Comparative protein structure modeling of genes and genomes. Annu Rev Biophys Biomol Struct 29:291–325
26. Sali A, Blundell TL (1993) Comparative protein modelling by satisfaction of spatial restraints. J Mol Biol 234:779–815
27. Fiser A, Do RK, Sali A (2000) Modeling of loops in protein structures. Protein Sci 9:1753–1773
28. MacKerell AD, Bashford D, Bellott M, Dunbrack RL, Evanseck JD, Field MJ, Fischer S, Gao J, Guo H, Ha S, Joseph-McCarthy D, Kuchnir L, Kuczera K, Lau FTK, Mattos C, Michnick S, Ngo T, Nguyen DT, Prodhom B, Reiher WE, Roux B, Schlenkrich M, Smith JC, Stote R, Straub J, Watanabe M, Wiorkiewicz-Kuczera J, Yin D, Karplus M (1998) All-atom empirical potential for molecular modeling and dynamics studies of proteins. J Phys Chem B 102:3586–3616
29. Kabsch W, Sander C (1983) Dictionary of protein secondary structure: pattern recognition of hydrogen bonded and geometrical features. Biopolymers 22:2577–2637
30. Frishman D, Argos P (1995) Knowledge-based protein secondary structure assignment. Proteins 23:566–579
31. Laskoswki RA, MacArthur MW, Moss DS, Thornton JM (1993) PROCHECK: a program to check the stereochemical quality of protein structures. J Appl Crystallogr 26:283–291
32. Wallner B, Elofsson A (2003) Can correct protein models be identified? Protein Sci 12:1073–1086
33. Pawlowski M, Gajda MJ, Matlak R, Bujnicki JM (2008) MetaMQAP: a meta-server for the quality assessment of protein models. BMC Bioinform 9:403
34. Schneidman-Duhovny D, Inbar Y, Nussinov R, Wolfson HJ (2005) PatchDock and SymmDock: servers for rigid and symmetric docking. Nucleic Acids Res 33:W363–W367
35. van der Spoel D, Lindahl E, Hess B, Groenhof G, Mark AE, Berendsen HJ (2005) GROMACS: fast, flexible, and free. J Comput Chem 26:1701–1718
36. van Gunsteren WF, Billeter SR, Eising AA et al (1996) Biomolecular asimulation: the GROMOS96 manual and user guide. ETH, Zürich
37. Berendsen HJC, Postma JPM, van Gunsteren WF, Hermans J (1981) Interaction models for water in relation to protein hydration. In: Pullman B (ed) Intermolecular forces. Reidel, Dordrecht
38. Berendsen HJC, Postma JPM, van Gunsteren WF, Di Nola A, Haak JR (1984) Molecular dynamics with coupling to an external bath. J Chem Phys 81:3684–3690
39. Darden T, York D, Pedersen L (1993) Particle mesh Ewald- an N. Log(N) method for Ewald sums in large systems. J Chem Phys 98:10089–10092
40. Hess B, Bekker H, Berendsen HJC, Fraaije JGEM (1997) LINCS: a linear constraint solver for molecular simulations. J Comput Chem 18:1463–1472
41. Wallace AC, Laskowski RA, Thornton JM (1995) LIGPLOT: a program to generate schematic diagrams of protein-ligand interactions. Protein Eng 8:127–134
42. Veerapandian B, Gilliland GL, Raag R, Svensson AL, Masui Y, Hirai Y, Poulos TL (1992) Functional implications of interleukin-1 beta based on the three-dimensional structure. Proteins 12:10–23
43. Schreuder H, Tardif C, Trump-Kallmeyer S, Soffientini A, Sarubbi E, Akeson A, Bowlin T, Yanofsky S, Barrett RW (1997) A new cytokine-receptor binding mode revealed by the crystal structure of the IL-1 receptor with an antagonist. Nature 386:194–200
44. Pettersen EF, Goddard TD, Huang CC, Couch GS, Greenblatt DM, Meng EC, Ferrin TE (2004) UCSF Chimera-a visualization system for exploratory research and analysis. J Comput Chem 25:1605–1612
45. Stone MJ (2001) NMR relaxation studies of the role of conformational entropy in protein stability and ligand binding. Acc Chem Res 34:379–388
46. Vigers GP, Dripps DJ, Edwards CK 3rd, Brandhuber BJ (2000) X-ray crystal structure of a small antagonist peptide bound to interleukin-1 receptor type 1. J Biol Chem 275:36927–36933
47. Koradi R, Billeter M, Wuthrich K (1996) MOLMOL: a program for display and analysis of macromolecular structures. J Mol Graph 14:51–55